Available online at www.sciencedirect.com
SCIENCE DIRECT®
Chemical Physics Letters 406 (2005) 345–350
CHEMICAL PHYSICS LETTERS
www.elsevier.com/locate/cplett

Time-resolved kinetic studies on quenching of HCCl($\tilde{A}^1A''(040)$) by alkane and alcohol molecules

Xueliang Yang, Yunzhen Liu, Hailing Wang, Yang Chen, Congxiang Chen *

Open Laboratory of Bond-selective Chemistry, Chinese Academy of Sciences, Department of Chemical Physics, University of Science and Technology of China, Hefei, Auhui 230026, PR China

Received 1 February 2005; in final form 28 February 2005
Available online 23 March 2005

Abstract

HCCl($\tilde{X}^1A'$) radicals were produced by laser photolysis of $HCClBr_2$ at 213 nm, and were electronically excited to $\tilde{A}^1A''(040)$ at 617.97 nm with a dye laser pumped by a Nd:YAG laser. Experimental quenching data of HCCl($\tilde{A}^1A''(040)$) by alkane and alcohol molecules were measured at room temperature (293 K) by observing the time-resolved total fluorescence signals in a cell where the total pressure was 23.0 Torr. It was shown that the quenching rate constant of HCCl($\tilde{A}^1A''(040)$) by alkane molecules increase almost linearly with the number of C–H bonds contained in the homologous molecules. The formation cross-sections of the complexes between HCCl($\tilde{A}^1A''$) and quenchers were calculated by means of collision complex model and the attractive forces between the collision partners were considered to play an important role in the quenching processes of HCCl($\tilde{A}^1A''(040)$) by the quenchers studied in this work.

1. Introduction

Due to their importance as intermediates in combustion, atmosphere and organic chemistry, simple carbenes such as methylene, CH_2, and halomethylenes, HCX, have been the subject of numerous experimental and theoretical investigations in the last few decades. As one of the important simple carbenes, HCCl has received significant attention. In 1966, Merer and Travis [1] reported the first rotationally resolved absorption spectra of HCCl between 550 and 820 nm in the flash photolysis of $HCClBr_2$, and henceforth, there have been some reports of rotationally resolved spectra in both near-infrared and visible wavelengths [2–17]. These spectra of HCCl show strong and complicated perturbations caused by Renner–Teller effects and spin–orbit couplings [1–9]. As for the dynamics of HCCl radicals, only the reactions of the ground state with NO, NO_2, O_2, C_2H_2, C_2H_4, and C_3H_6 [18–20] have been studied in the last decades, while there is not any report about the kinetics of excited state $\tilde{A}^1A''$ until now.

In the present work, HCCl($\tilde{X}^1A'$) radical was produced by laser photolysis of $HCClBr_2$ at 213 nm. The quenching rate data of HCCl($\tilde{A}^1A''(040)$) by alkane and alcohol molecules were obtained for the first time reported by measuring the time-resolved fluorescence signals of the excited state at room temperature.

2. Experimental

The pulsed laser photolysis/laser-induced fluorescence (LP-LIF) experiments were performed in a stainless steel flow reactor, which is similar to that described in details previously [21]. Briefly, HCCl radicals were generated by the photolysis of $HCClBr_2$ with a focused 213 nm irradiation of a frequency-quintupled

* Corresponding authors. Fax: +86 551 3602969.
E-mail address: cxchen@ustc.edu.cn (C. Chen).

0009-2614/$ - see front matter © 2005 Elsevier B.V. All rights reserved.
doi:10.1016/j.cplett.2005.03.014

Nd:YAG laser (New wave, repetition rate of 10 Hz). A 35 cm focal length quartz lens focused the beam into the center of the reaction cell. After a time delay, the ground state HCCl($\tilde{X}^1A'$) was excited to the $\tilde{A}^1A''$ state with a dye laser beam (Sirah) pumped by Nd:YAG laser (Spectra physics, GCR-170, repetition rate of 10 Hz). The excitation laser and the photolysis laser beams overlapped in the reaction cell collinearly in a counter propagating way. And the typical output pulse energies of them were 4 and 3 mJ, respectively. In order to minimize scattering light, the laser beams were passed through a set of special light baffles. The fluorescence signals of the excited HCCl were collected by a photomultiplier (GDB56, Beijing) through a cutoff filter with wavelengths longer than 685 nm and the outputs of the photomultiplier were recorded by a digital storage oscilloscope (TDS380, Tektronix) or a transient digitizer and averaged with a computer data acquisition system over 512 laser shots. A multi-channel digital delay generator (Stanford Research DG535) controlled the time delay between the photolysis laser and the excitation dye laser beam.

In the typical experiments, the premixed gas samples containing $CHClBr_2$ molecule as the HCCl radical precursor and the quenchers mixed with Ar as buffer gas, supplied from different reservoirs, controlled and measured by an individually calibrated mass flow meter (D07-7A/2M, Beijing), slowly passed through the reaction cell. The typical concentration of $CHClBr_2$ was 3.0×10^{13} molecule cm^{-3}, while the concentrations of alkane and alcohol molecules varied in the range from 1.0×10^{14} up to 5.0×10^{15} molecule cm^{-3}. To keep the concentration of HCCl radical constant, the concentrations of $CHClBr_2$, the total pressure (23.0 Torr), photolysis laser energy and the delay time were kept constant in all experiments. The nascent HCCl radicals generated from the photolysis of the precursor are vibrationally and rotationally hot. Ar buffer gas in the reaction mixture serves not only to relax the nascent quantum state distributions of the HCCl radicals but also to slow down the diffusion of molecules from the detection region.

2.1. Materials

In this work, $HCClBr_2$ (Aldrich Chemical Company, 98.0%), methane (Nanjing gas 99.9%), ethane (Nanjing gas 99.99%), propane (Nanjing gas, 99.9%), *n*-butane (Nanjing gas, 99.9%), *n*-hexane (Tianjin, >99.9%), *c*-hexane (Shanghai, >99.5%), *n*-octane (Shanghai, >97.5%), methanol (Jiangsu, >99.5%), ethanol (Shanghai, >99.5%), *n*-propanol (Shanghai, >99.0%), *n*-butanol (Shanghai, >99.5%) and *n*-hexyl alcohol (Hangzhou, >99.0%) were degassed by repeated freeze–pump–thaw cycles in liquid nitrogen. Ar (Nanjing gas 99.999%) was used without further purification.

3. Results

A portion of the LIF excitation spectrum of HCCl recorded at 15 μs delay after the photolysis of $CHClBr_2$ in the presence of 23.0 Torr argon at room temperature over the wavelength range of 15 100–16 660 cm^{-1} is depicted in Fig. 1. The 15 μs delay was chosen to minimize the effects of the scattered light and to allow the thermalization of the nascent HCCl. The spectrum agrees well with the work observed in earlier years [1,2,4] and it can be readily assigned to be the K structure of $\tilde{A}^1A''(030)\leftarrow\tilde{X}^1A'(000)$ and $\tilde{A}^1A''(040)\leftarrow\tilde{X}^1A'(000)$ transitions of the HCCl transient.

The excitation dye laser, operating with R610 at 617.97 nm (16 182 cm^{-1}), was used to pump the *Q* subband of $\tilde{A}^1A''(04^20)\leftarrow\tilde{X}^1A'(000)$ transition. The time resolved fluorescence signal of HCCl($\tilde{A}^1A''(040)$) quenched by n-C_4H_{10} is illustrated in Fig. 2a. The nature of the exponential decays is demonstrated by the semilogarithmic plots in Fig. 2b, where the solid line is the result of linear least squares fitting corresponding to more than a 100 ns delay from the maximum point to reduce the disturbance caused mainly by laser scattering light. These plots clearly show a single exponential decay curve. The experimentally monitored decay curve was fitted to

$$I = I_0\exp(-k't), \tag{1}$$

where k' is a first-order rate coefficient. The values of k' at different partial pressures of quencher were derived from similar plots as those illustrated in Fig. 2. In the experiments, there are background gases (including argon, $CHClBr_2$, and some other photolysis fragments) beside the quenchers. Therefore the first-order rate coefficient k' should be expressed as

$$k' = k_q[Q] + \sum_i k_i[M_i] + k_f. \tag{2}$$

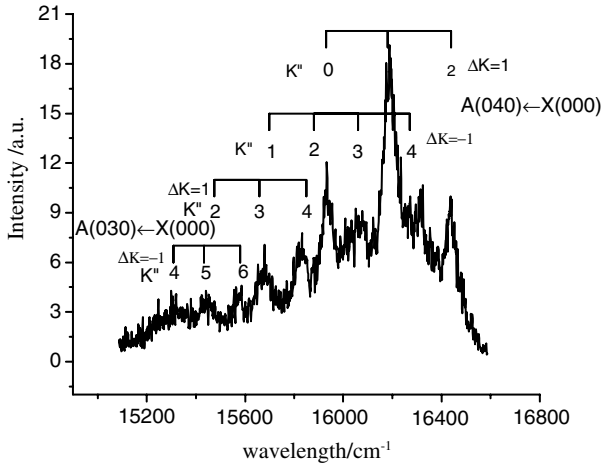

Fig. 1. The LIF spectrum of HCCl obtained 15 μs delay after 213 nm photolysis of $CHClBr_2$ under the pressure of 23.0 Torr at 293 K.

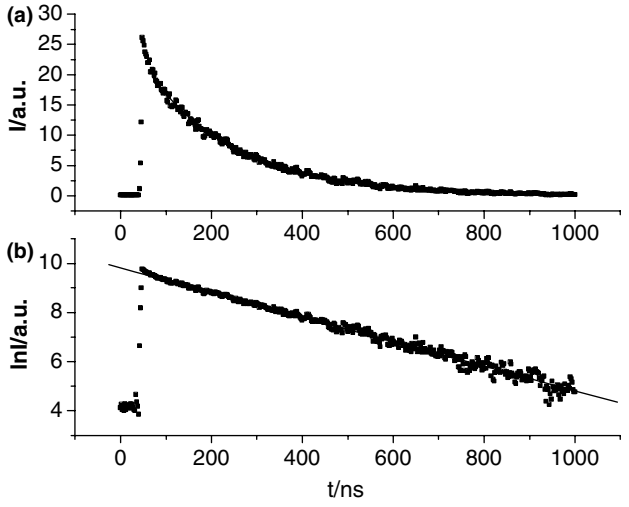

Fig. 2. The typical time-resolved fluorescence decay signal of HCCl($\tilde{A}^1A''(040)$) with C_4H_{10} (a) and its semi-logarithmic plot (b) at 617.97 nm under the pressure of 23.0 Torr at 293 K. (■) experimental data and (–) fitting result the concentration of C_4H_{10} is about 6.6×10^{14} molecule cm^{-3}.

Here, k_q represents the rate constant of the chemical reaction of HCCl($\tilde{A}^1A''(040)$) with the quencher (denoted as Q) and the transition of $\tilde{A}^1A''(040) \rightarrow \tilde{X}^1A'$ caused by collision with Q. k_i is the collision quenching constant of HCCl($\tilde{A}^1A''(040)$) by the background gases, and k_f represents the Einstein spontaneous emission coefficient from A to X. In the present work, the background gases and total pressure were constant in all experiments. So the first-order rate coefficient is proportional to the concentration of the added quenchers, and the slope coefficient is the quenching rate constant k_q and the intercept is the sum of the contribution of various background gases and Einstein spontaneous emission coefficient k_f, as shown in Fig. 3.

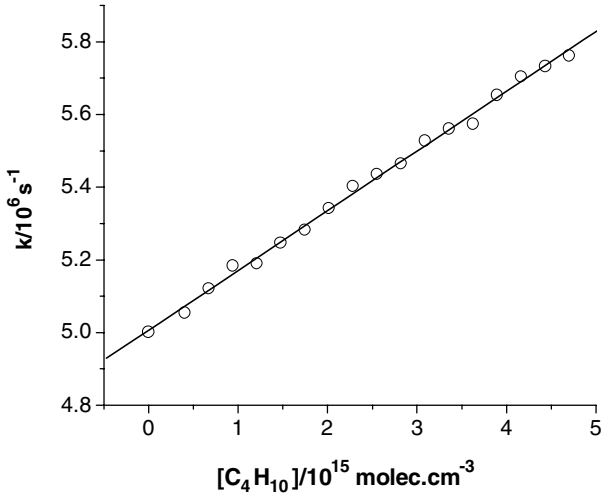

Fig. 3. Plot of the first-order rate constant for quenching of HCCl($\tilde{A}^1A''(040)$) as a function of concentration of C_4H_{10}.

Table 1
Quenching rate constants k_q and cross-sections σ_q of HCCl($\tilde{A}^1A''(040)$) radicals by the alkane and alcohol molecules measured in this work at 293 K

Quencher	$k_q/10^{-10}$ cm^3 $molec^{-1}$ s^{-1}	$\sigma_q/10^{-2}$ nm^2
CH_4	⩽0.18	⩽2.51
C_2H_6	0.58 ± 0.04	10.1 ± 0.7
C_3H_8	1.12 ± 0.14	21.7 ± 2.8
n-C_4H_{10}	1.54 ± 0.20	31.9 ± 4.1
n-C_6H_{14}	3.40 ± 0.27	75.1 ± 6.0
n-C_6H_{14}	2.72 ± 0.22	61.0 ± 4.9
c-C_6H_{12}	2.23 ± 0.34	49.8 ± 7.6
n-C_8H_{18}	3.67 ± 0.37	86.3 ± 8.7
CH_3OH	3.12 ± 0.37	55.2 ± 6.5
C_2H_5OH	3.80 ± 0.35	74.4 ± 6.8
n-C_3H_7OH	4.53 ± 0.38	94.5 ± 7.9
n-C_4H_9OH	5.38 ± 0.52	117.3 ± 11.3
n-$C_6H_{13}OH$	6.50 ± 0.54	150.1 ± 12.5

The measured quenching rate constants are converted to effective quenching cross-sections, σ_q, by the relation

$$\sigma_q = k_q/\langle v \rangle, \tag{3}$$

where the averaged relative kinetic velocity is

$$\langle v \rangle = (8kT/\pi\mu)^{1/2}. \tag{4}$$

Here, k is the Boltzmann constant, T is the absolute temperature, and μ is the reduced mass of the collision partners. A summary of the observed quenching rate coefficients and cross-sections are given in Table 1. The data in Table 1 are quoted with 2σ experimental estimates for the uncertainty.

4. Discussion

The quenching process of the excited state radical is very complicated, involving not only physical quenching but also chemical reaction. As has been indicated in earlier years [22], rotational and translational relaxations of the nascent HCCl are accomplished on time scales much more rapidly than the delay time employed in this investigation. Further, the time-resolved fluorescence decay signals show clearly single exponential decay curve, indicating that the contributions from collisionally induced inter-system crossing between $\tilde{A}^1A''$ and $\tilde{a}^3A''$ to the total removal of HCCl($\tilde{A}^1A''(040)$) may be neglected. Moreover, the possibilities of vibrational energy transfer are expected to be basically smaller than 1/100 since there is no resonance state between the collision partners, thus the contribution from vibrational relaxation is negligible [22]. Hence, the reactive quenching and electronic quenching may be the predominant channel for the rapid processes observed in this work.

It can be seen in Table 1 that the quenching rate constants of HCCl($\tilde{A}^1A''(040)$) by alcohol and alkane molecules increase steadily with the number of C atoms

contained in these homologous molecules, while the quenching of HCCl($\tilde{A}^1A''(040)$) by alcohol is much more effective than that by the corresponding alkane molecule. This result is very similar to the results of CCl_2, which has been investigated in our lab [23].

The quenching cross-sections of HCCl($\tilde{A}^1A''(040)$) by alkanes and alcohols are very large and have the same magnitude as those proposed by hard sphere collision model, indicating the role of the long range attractive forces between HCCl($\tilde{A}^1A''(040)$) and the collision partners in the entrance channel of the quenching processes. In the collision complex model proposed by [24–27], the collision partners will form an excited state complex resulting from the long-range multipole attractive forces. During the residence time the complex will dissociate to electronic ground state HCCl($\tilde{X}^1A'$) and the quenchers through the energy transfer in different vibrational freedoms, form products by chemical reaction, or dissociate back to the collision partners themselves. The scheme of the process can be expressed as follows:

$$\mathrm{HCCl}(\tilde{A}) + Q \underset{k_{-1}}{\overset{k_1}{\leftrightarrow}} [\mathrm{HCCl}(\tilde{A}) - Q]^* \overset{k_{q_1}}{\rightarrow} \mathrm{HCCl}(\tilde{X}) + Q, \quad (5)$$

$$\overset{k_{q_2}}{\rightarrow} \mathrm{Product}. \quad (6)$$

The effective attractive potential in the collision process could be expressed using the most favorable orientation method as [24]:

$$V_{\mathrm{eff}} = \frac{Eb^2}{R^2} - \frac{C_3}{R^3} - \frac{C_4}{R^4} - \frac{C_6}{R^6} - \frac{C'_6}{R^6}$$

or using the averaged orientation method [28]:

$$V_{\mathrm{eff}} = \frac{Eb^2}{R^2} - \frac{C_6}{R^6} - \frac{C_8}{R^8} - \frac{C'_6}{R^6} - \frac{C''_6}{R^6},$$

where E is the initial kinetic energy at infinite separation, b is the impact parameter, and R is the distance between the centers of masses of the HCCl($\tilde{A}^1A''(040)$) and the quenching partner. The C_n coefficients represent the attractive terms due to multiple interactions corresponding to dipole–dipole, dipole–quadrupole, and dipole-induced dipole and dispersion forces, respectively. Expressions for these values are given in [25,28]. In a collision at a particular kinetic energy E, there exists an impact parameter b_0 at which the maximum of the effective potential is just equal to E and only for $b < b_0$ the collision complex between collision partners can be formed. So the cross-section for complex formation at this kinetic energy can be expressed as

$$\sigma_{\mathrm{eff}}(E) = \pi b_0^2(E).$$

Thus, the thermally averaged complex formation cross-section at temperature T is

$$\sigma_{\mathrm{eff}} = \frac{1}{(kT)^2} \int_0^\infty \sigma'_{\mathrm{eff}}(E) \cdot E \cdot \exp\left(-\frac{E}{kT}\right) \mathrm{d}E.$$

The quenching cross-sections σ_q observed in the experiments includes the outcomes (5) and (6), thus it is equal to that of complex formation times a probability P, viz., $\sigma_q = P \cdot \sigma_{\mathrm{eff}}$, where

$$P = \frac{k_{q_1} + k_{q_2}}{k_{-1} + k_{q_1} + k_{q_2}}. \quad (7)$$

The values for the dipole moments μ, quadrupole moments Q, polarizabilities α and ionization potentials IP of HCCl($\tilde{A}^1A''$) and collision partners required for the calculation are given in Table 2 together with the resulting cross-sections for complex formation and the probability P at 293 K. The values of the appropriate molecular parameters were taken from various literature sources (see Table 2) and those of HCCl($\tilde{A}^1A''$) were computed at UMP2(full)/6-311++G(3df,2p) level with GAUSSIAN 98 package [29] which can give a well description of the excited state HCCl($\tilde{A}^1A''$).

As is shown in Table 2, the dipole moment of alcohol is usually much larger than that of the corresponding alkane so that the long range attractive force between HCCl($\tilde{A}^1A''(040)$) and alcohol is much stronger than that between HCCl($\tilde{A}^1A''(040)$) and alkane. According to collision complex model, the complex formation cross-sections between HCCl($\tilde{A}^1A''(040)$) and alcohols would be much larger than those for alkanes. Therefore, it can be seen the alcohols are much effective than the alkanes for the quenching of HCCl($\tilde{A}^1A''(040)$). Table 2 also shows that the probabilities P for alcohols are generally larger than those for alkanes and they both increase with increasing number of C atom contained in the analogous molecules.

For the quenching process of the electronically excited radical HCCl($\tilde{A}^1A''(040)$), the total available energy of the collision complex is mainly contributed by the energy of HCCl($\tilde{A}^1A''(040)$) because it is much larger than that of the alkane or alcohol molecule. Therefore, it can be considered that the total available energies of the complexes are similar. During the residence time of the complex, the energy will be redistributed among the various internal freedoms. When the complex dissociates to form physical quenching products, the E–V energy transfer will occur between HCCl($\tilde{A}^1A''(040)$) and the vibrational state of the quencher. Generally, the increasing number of normal modes accompanying the increase in the number of C atoms in the analogous molecules results in the higher state density and probability of energy transfer. For a given total energy, it can be expected that the rate constant k_{q_1} will be bigger for a larger molecule than that for an analogous smaller one.

The singlet carbenes generally undergo indiscriminate insertion into C–H bonds [34,35] besides physical quenching on collision with saturated hydrocarbon. Generally, the rate constant of insertion reaction does not exhibit marked variations with the type of C–H

Table 2
Calculated complex formation cross-sections σ_{cf} of HCCl($\tilde{A}$) with quenchers and parameters used in the calculations (α in 10^{-24} cm^3 and Q in 10^{-26} esu · cm^3) at 293 K

Quencher	μ(D)[a]	α[a]	Q[b]	IP[a] (eV)	σ_q (10^{-2} nm^2)	Calc. σ_{cf} (10^{-2} nm^2)			
						Max.[c]	P	Ave.[d]	P
CH_4	0.00	2.59	0.00	12.63	⩽2.52	92.0	0.03	86.9	0.03
C_2H_6	0.00	4.47	0.65	11.52	10.1	112.4	0.09	103.1	0.10
C_3H_8	0.08	6.37	1.50	10.94	21.7	132.4	0.16	115.6	0.19
n-C_4H_{10}	0.03	8.20	2.00	10.53	31.9	141.7	0.23	125.2	0.26
n-C_6H_{14}	0.05	11.9	3.00	10.13	61.0	161.8	0.38	141.2	0.43
c-C_6H_{12}	0.00	11.0	0.90	9.80	49.8	147.5	0.34	136.1	0.37
n-C_8H_{18}	0.08[e]	15.9[e]	3.90[e]	9.88[e]	86.3	179.4	0.48	155.2	0.56
CH_3OH	1.70	3.29	0.50	10.84	55.2	185.2	0.30	109.7	0.50
C_2H_5OH	1.69	5.11	1.65	10.49	74.4	198.0	0.38	120.4	0.62
n-C_3H_7OH	1.68	6.74	2.40	10.22	94.5	206.8	0.46	128.5	0.74
n-C_4H_9OH	1.66	8.88	3.00	9.99	117.3	215.4	0.54	137.5	0.85
n-$C_6H_{13}OH$	1.63[e]	12.4[e]	3.90[e]	9.80[e]	150.1	227.7	0.66	150.3	1.00
HCCl(Ã)	0.90[f]	5.71[f]	1.61[f]	7.84[g]					

[a] Ref. [30].
[b] Ref. [31].
[c] Calculated using the most favorable orientation method.
[d] Calculated using the averaged orientation method.
[e] Estimated following [23,32] and other analogous molecule.
[f] Computed with GAUSSIAN 98 at UMP2(full)/6-311++G(3DF,2P) level.
[g] Ref. [33].

bond involved [23,34,35]. As is plotted in Fig. 4, the rate constants of HCCl($\tilde{A}^1A''(040)$) by alkane and alcohol molecules increase almost linearly with the number of C–H bonds contained in the analogous molecules and there are no remarkable variations between the C–H bonds in CH_3 or CH_2 groups, which is consistent with the insertion mechanism. The insertion of HCCl($\tilde{A}^1A''(040)$) into C–H bonds of alcohols will be easier because of the induction of OH substitute. Thus, the rate constants k_{q_2} with alcohols are expected to be larger than those with alkanes.

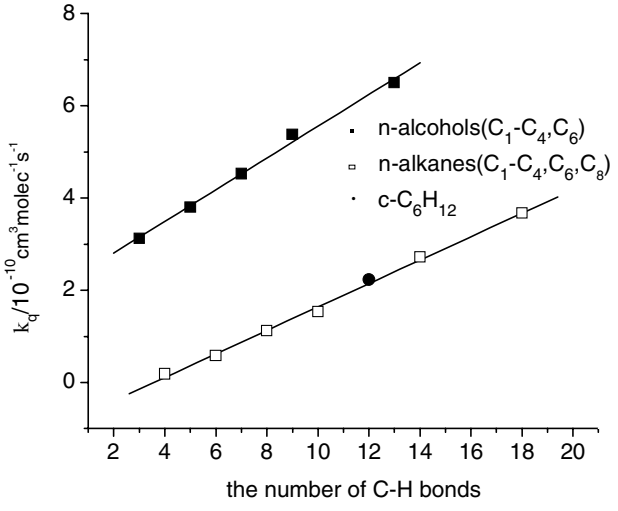

Fig. 4. The dependence of the experimental rate constants k_q for quenching of HCCl($\tilde{A}^1A''(040)$) by the quenchers on the number of C–H bonds contained in these molecules.

Since the total available energy of the complexes are similar, it can be expected that the rate constant k_{-1} will decrease with the increasing attractive forces between the collision partners in the complexes, while k_1 will turn larger. For the complex formed between HCCl($\tilde{A}^1A''(040)$) and alkanes, the dipole-induced dipole and dispersion forces play a main role and they will turn larger with the number of C atoms contained in the quenchers. Thus k_{-1} will decrease while k_1 increase with the size of the molecules. And there is the same trend for the alcohols, where the dipole–dipole interactions are more important and almost kept constant.

According to Eq. (7), the quenching rate constants and the possibilities (P) would exhibit the behavior as shown in Tables 1 and 2, respectively. Based on all above analysis, we considered that the quenching of HCCl($\tilde{A}^1A''(040)$) by alkanes and alcohols are likely to form collision complexes due to the long range attractive forces between the collision partners, then dissociate to quenching products via E–V energy transfer and insertion chemical reaction.

5. Conclusion

In this work, the quenching rate constants of HCCl($\tilde{A}^1A''(040)$) by alkane and alcohol molecules were measured by the LP-LIF experiments. They grow up almost linearly with the increase of the number of C atoms contained in the analogous molecules. With the application of the collision complex model, the attractive forces

between the collision partners were demonstrated to play an important role in the quenching of HCCl($\tilde{A}^1A''(040)$) by these molecules and the quenching process may include E–V energy transfer in the collision complex and insertion reaction.

Acknowledgments

This work was financially supported by the China National Key Basic Research Special Foundation (G1999075304), the National Natural Science Foundation of China (10032050, 20373065, 20328305), and Chinese Academy of Science(KJCX2-SW-H08).

References

[1] A.J. Merer, D.N. Travis, Can. J. Phys. 44 (1966) 525.
[2] M.E. Jacox, D.E. Milligan, J. Chem. Phys. 47 (1967) 1626.
[3] M. Kakimoto, S. Saito, E. Hirota, J. Mol. Spectrosc. 97 (1983) 194.
[4] Y. Qiu, S. Zhou, J. Shi, Chem. Phys. Lett. 136 (1987) 93.
[5] M.K. Gilles, K.M. Ervin, J. Ho, W.C. Lineberger, J. Phys. Chem. 96 (1992) 1130.
[6] S. Xu, K.A. Beran, M.D. Harmony, J. Phys. Chem. 98 (1994) 2742.
[7] B.-C. Chang, T.J. Sears, J. Chem. Phys. 102 (1995) 6347.
[8] B.-C. Chang, T.J. Sears, J. Mol. Spectrosc. 173 (1995) 391.
[9] B.-C. Chang, R. Fei, T.J. Sears, J. Mol. Spectrosc. 183 (1997) 341.
[10] B.-C. Chang, T.J. Sears, J. Chem. Phys. 105 (1996) 2135.
[11] B.-C. Chang, M.L. Costen, A.J. Marr, G. Ritchie, G.E. Hall, T.J. Sears, J. Mol. Spectrosc. 202 (2000) 131.
[12] A. Lin, K. Kobayashi, H.-G. Yu, G.E. Hall, J.T. Muckerman, T.J. Sears, A.J. Merer, J. Mol. Spectrosc. 214 (2002) 216.
[13] C.-W. Chen, T.-C. Tsai, B.-C. Chang, Chem. Phys. Lett. 347 (2001) 73.
[14] C.-L. Lee, M.-L. Liu, B.-C. Chang, J. Chem. Phys. 117 (2002) 3263.
[15] H. Fan, I. Ionescu, C. Annesley, J. Cummins, M. Bowers, S.A. Reid, J. Mol. Spectrosc. 225 (2004) 43.
[16] C.-S Lin, Y.-E. Chen, B.-C. Chang, J. Chem. Phys. 121 (2004) 4164.
[17] B. Hajgato, H.M.T. Nguyen, T. Veszpremi, M.T. Nguyen, Phys. Chem. Chem. Phys. 2 (2000) 5041.
[18] R. Wagener, H.Gg Wagner, Z. Phys. Chem. 9 (1992) 1755.
[19] H.-H. Carstensen, C. Pehbein, H.Gg Wagner, Ber. Bunsenges. Phys. Chem. 101 (1997) 1429.
[20] R.E. Baren, M.A. Erickson, J.F. Hershberger, Int. J. Chem. Kinet. 34 (2002) 12.
[21] Y.-Z. Liu, Z.-Q. Zhang, L.-S. Pei, Q. Ran, Y. Chen, C.-X. Chen, Chem. Phys. 303 (2004) 255.
[22] R.D. Levine, R.B. Bernstain, Molecular Reaction Dynamics, Oxford University Press, Oxford, 1974.
[23] Y.-D. Gao, Ph.D. Thesis, University of Science and Technology of China, 2001.
[24] P.W. Fairchild, G.P. Smith, D.R. Closley, J. Chem. Phys. 79 (1983) 1795.
[25] J.C. Trully, J. Chem. Phys. 61 (1974) 61.
[26] G.E. Zahr, R.K. Preston, W.H. Miller, J. Chem. Phys. 62 (1975) 1127.
[27] D.L. Holtermann, E.K.C. Lee, R. Nanes, J. Chem. Phys. 77 (1982) 5327.
[28] J.O. Hirschfelder, C.F. Curtis, R.B. Bird, Molecular Theory of Gases and Liquids, Wiley, New York, 1954, p. 26.
[29] M.J. Frisch et al., Gaussian 98, Revision A.7, Gaussian Inc., Pittsburgh, PA, USA, 1998.
[30] R-C. Weast, CRC Handbook of Chemistry and Physics, 80th edn., CRC, Boca Raton, FL, 1999 (Chapter 9).
[31] D.D. Stogryn, A.P. Stogryn, Mol. Phys. 11 (1966) 371.
[32] R.A. Copeland, M.J. Dyer, D.R. Closley, J. Chem. Phys. 82 (1985) 4022.
[33] S.G. Lias, Z. Karpas, J.F. Liebman, J. Am. Chem. Soc. 107 (1985) 6089.
[34] C. Wentrup, Reactive Molecules, Wiley-Interscience, NewYork, 1984.
[35] M. Kirmse (Ed.), Carbene Chemistry, 2nd edn., Academic Press, New York, 1971.